Advanced Turbomachinery Components for Supercritical CO2 Power Cycles
Final Technical Report
Project period October 2014 through March 2016
March 31, 2016
DOE Award # DE-FE0023998

PI: Michael McDowell
michael.mcdowell@gastechnology.org
818-405-9548
818-813-2733 Cell

Gas Technology Institute
5945 Canoga Ave.
Woodland Hills, CA 91367
DUNS Number 045060753

Subcontractors:
Electric Power Research Institute (Palo Alto, California)
Duke Energy (Charlotte, North Carolina)
Alstom (Knoxville, Tennessee)
The Oak Ridge National Laboratory (Oak Ridge, Tennessee)

Submitting Official

Michael McDowell PI

Acknowledgment: "This material is based upon work supported by the Department of Energy under Award Numbers DE-FE0023998."

Abstract

Six indirectly heated supercritical CO2 (SCO2) Brayton cycles with turbine inlet conditions of 1300°F and 4000 psia with varying plant capacities from 10MWe to 550MWe were analyzed. 550 MWe plant capacity directly heated SCO2 Brayton cycles with turbine inlet conditions of 2500°F and 4000 psia were also analyzed. Turbomachinery configurations and conceptual designs for both indirectly and directly heated cycles were developed. Optimum turbomachinery and generator configurations were selected and the resulting analysis provides validation that the turbomachinery conceptual designs meet efficiency performance targets. Previously identified technology gaps were updated based on these conceptual designs. Material compatibility testing was conducted for materials typically used in turbomachinery housings, turbine disks and blades. Testing was completed for samples in unstressed and stressed conditions. All samples exposed to SCO2 showed some oxidation, the extent of which varied considerably between the alloys tested. Examination of cross sections of the stressed samples found no evidence of cracking due to SCO2 exposure.

Table of Contents

1 Indirect Cycle Analysis

Approach: Six cases were analyzed using ASPEN. All six cases have a turbine inlet temperature of 1300°F and inlet pressure of 4000 psia, and all cases were configured as recompression cycles with a single pass through the heat source. The plant capacities analyzed were 10, 25, 50, 100, 250, and 550 MWe. The objective was to determine the optimum turbine design for each specified plant size.

1.1 System Analysis

Approach: Initial cycle analysis was performed with turbomachinery isentropic efficiencies held constant at 90% for the turbines and 85% for the compressors for all power levels. A single turbine element was used in the ASPEN model since, in turbomachinery configurations that use two turbines, they are arranged in parallel, and this approach is adequate to predict overall cycle performance. The 10 MWe (representing the smallest viable pilot plant scale) and 550 MWe plant sizes were chosen for turbomachinery sizing. The system models were then updated with the predicted turbomachinery efficiencies.

Results/Discussion: The process flow diagram for the 550 MWe plant is shown in Figure 1. The SCO2 is heated in the heat source heat exchanger (stream 1-2). It then gets expanded in the turbine (stream 3-4) and passes through the high temperature recuperator (stream 5-6) and the low temperature recuperator (stream 7-8). The fluid is then split between the main and recycle compressors, and the main compressor stream cooled to 90°F. The fluid then goes through recuperative heating to capture as much heat as possible before re-entering the heat source heat exchanger. The other plant capacity configurations are similar to the figure shown below; they differ only in the mass flow rate of the system.

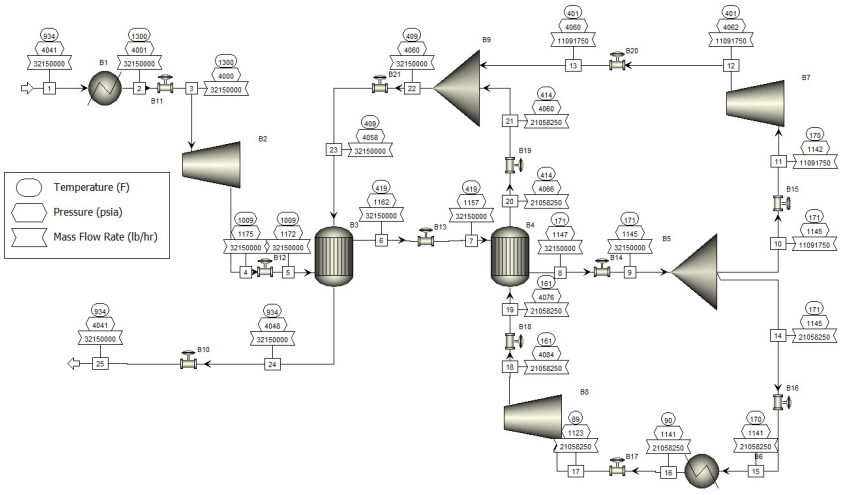

Figure 1. Process Flow Diagram for 550 MWe Indirectly Heated Cycle

1.2 Turbomachinery Analysis

Approach: Boundary conditions for the turbomachinery were taken from the system model. One dimensional sizing tools were used to optimize performance within appropriate design constraints. Variable design parameters for the compressors include: compressor rotational speed, head coefficient, flow coefficient, and hub to eye diameter ratio. Design constraints include: eye to tip diameter ratio, diffusion ratio, and impeller suction side pressure. The design parameters were varied within allowable ranges to optimize compressor performance. For the turbines, the fewest number of stages was chosen that still maintained acceptable efficiency to reduce complexity. The power bending stress on the blade and the pitch line velocity were evaluated to ensure they met design criteria.

Two turbomachinery configurations were evaluated: a single shaft configuration and dual shaft configuration. With the single shaft configuration, there is single turbine driving both the generator and the compressors. With the dual shaft configuration, there is a power turbine on its own shaft and a compressor turbine, along with two compressors, on a second shaft.

Results/Discussion: Detailed information of each configuration is shown below in Tables 1 and 2. Four stage, split flow, back-to-back turbine configurations were chosen in each case to minimize rotor blade power bending loads, and to better manage axial thrust. For the 550 MWe plant size, the power turbine speed is synchronous with the generator at 3600 RPM. In the single shaft configuration, the compressors run on the same shaft, and so also rotate at 3600 rpm. In the dual shaft configuration, the compressors optimize at a higher rotational speed of 6000 RPM,

resulting in better compressor performance, and leading to higher cycle efficiency. Thus, the dual shaft case was chosen for the turbomachinery layout.

Turbine Concept	Turbine (MW)	Turbine Efficiency	Power Turbine RPM	Main Compressor (MW)	Main Compressor Efficiency	Recycle Compressor (MW)	Recycle Compressor Efficiency	Compressor (and Compressor Turbine) RPM	Net Power (MW)	Mass Flow Rate (lb/hr)	Cycle Efficiency
Single Shaft	806.5	0.901	3600	102.27	0.781	154.41	0.711	3600	550	33,600,000	51.03%
Dual Shaft	770.83	0.9	3600	89.23	0.85	131.67	0.802	6000	550	32,150,000	52.62%

Table 1. Dual vs Single Shaft Evaluation for Indirectly Heated Cycle at 550 MWe

For the 10 MWe plant size, the power turbine can operate at much higher speeds as the power is low enough for it to be attached to the generator through a gearbox. In the single turbine configuration, the compressor rotational speed optimizes at a much higher speed than the turbine, and so the mechanical connection between the two will be through a gearbox. Alternatively, the compressors could be driven by an electric motor using power generated by the turbine. The dual shaft configuration allows for higher compressor rotational speeds, which leads to a slightly higher cycle efficiency. Thus, the dual shaft case was also chosen for the 10MWe turbomachinery layout. This choice has the added advantage that the 10MWe system configuration is directly traceable to large commercial size power plant configurations.

Turbine Concept	Turbine (MW)	Turbine Efficiency	Power Turbine RPM	Main Compressor (MW)	Main Compressor Efficiency	Recycle Compressor (MW)	Recycle Compressor Efficiency	Compressor (and Compressor Turbine) RPM	Net Power (MW)	Mass Flow Rate (lb/hr)	Cycle Efficiency
Single Shaft	14.72	0.8585	20000	1.95	0.797	2.79	0.767	39600	10	638,000	48.84%
Dual Shaft	14.67	0.854	25000	1.92	0.798	2.73	0.769	40000	10	663,000	49.83%

Table 2. Dual vs Single Shaft Evaluation for Indirectly Heated Cycle at 10 MWe

1.3 Turbomachinery Design

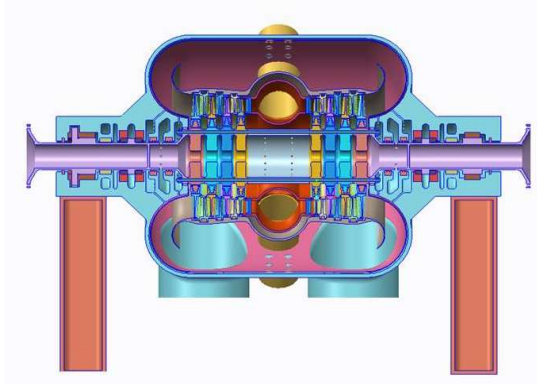

Figure 2. 550MWe Indirect Cycle Turbine Configuration

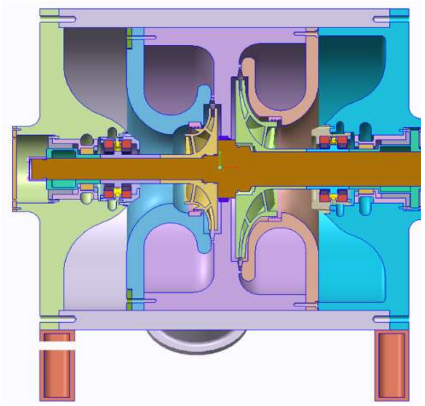

Figure 3. Indirect Cycle Compressor Configuration

Approach: Conceptual designs were developed using the sizing calculated in the analysis task, and design practices developed for high power density rocket engine turbomachinery.

Results/Discussion: Figures 2 and 3 below show the layouts for the 550 MWe turbomachinery. The two turbines are identical in configuration, and so only the compressor turbine is shown here. The 10 MWe equipment is similar in design, but differs in size to the 550 MWe.

2 Direct Cycle Analysis

Approach: Six cases were analyzed as shown in Table 3. All cases have a turbine inlet temperature of 2500°F and pressure of 4000 psia with a 550 MWe plant capacity. All systems were configured as simple Brayton cycles, with a single compressor, single recuperator and the remaining heat in the flue gas driving a bottoming cycle.

Case	Fuel	Coolant
1	Natural Gas	H2O
2	Syngas (91 mole% H2)	H2O
3	Syngas (39 mole% H2)	H2O
4	Natural Gas	CO2
5	Natural Gas	CO2 (closed loop coolant)
6	Syngas (39 mole% H2)	CO2 (closed loop coolant)

Table 3 Directly Heated Cycles Analyzed

2.1 System Analysis

Approach: Syngas (with both 31% and 91% hydrogen based on cases 1 and 2 in the DOE report 2010/1397) and natural gas were considered as fuels. Two different turbine blade coolants were used: H2O and CO2, and, where possible both rotors and stators were regeneratively cooled, with the heat captured in the coolant used elsewhere in

the cycle to improve efficiency. For the cases with CO2 as the coolant, two different cooling schemes were analyzed. In one scheme, the CO2 used for regenerative cooling was split from the recycle flow. In the other scheme, the regenerative coolant is in a separate closed loop.

Turbomachinery isentropic efficiencies of 90% for the turbines and 85% for the compressor were used in the initial analysis. The cycle performance was updated with predicted turbomachinery efficiencies after the sizing was complete. The bottoming cycle efficiency varied from 36-37.5% based on a curve fit of steam Rankine turbine inlet temperatures with steam cycle efficiencies. Pressure drop in piping and components was included.

Results/Discussion: The initial analysis showed all cases have similar cycle efficiencies; the difference among these cases is in the plant efficiency. The natural gas cases have plant efficiencies around 67% while the syngas cases have plant efficiencies around 48%. This low plant efficiency for the syngas cases is due to the large auxiliary loads of the gasification process. Thus, natural gas was chosen as the fuel source. CO2 was chosen as the turbine blade coolant as there wasn't much difference in system performance between H2O and CO2 turbine blade cooling, and the CO2 system is simpler. Between the two natural gas cases with CO2 as the coolant, the case with CO2 regenerative coolant in a separate loop was chosen.

The process flow diagram for the NG case with the CO2 regenerative blade coolant in a separate loop is shown in Figure 4. NG is preheated by the turbine blade coolant, and combusted with oxygen in combustor B25. Recycled CO_2 is added to the combustor to moderate the temperature (stream 32). The turbine is simulated as two separate turbines (B18 and B20) with film cooling entering at stream 20 and heat exchanger B10 simulating the regenerative cooling. The flue gas then enters the recuperator in which some heat is recovered by the recycled CO2. It then goes through the bottoming cycle heat exchanger (B5) where it is cooled down to 150°F. Water is removed from the system and the stream is cooled further to 90°F. It is then compressed back up to system pressure (stream 15). Some of the CO2 is removed for sequestration (stream 24), some is sent for film cooling of the turbine (stream 23) and the remainder is recycled back to the combustor (stream 31). A separate closed loop of CO2 is used for regenerative cooling of the turbine. Final cycle efficiencies with updated turbomachinery efficiencies are shown in Table 4.

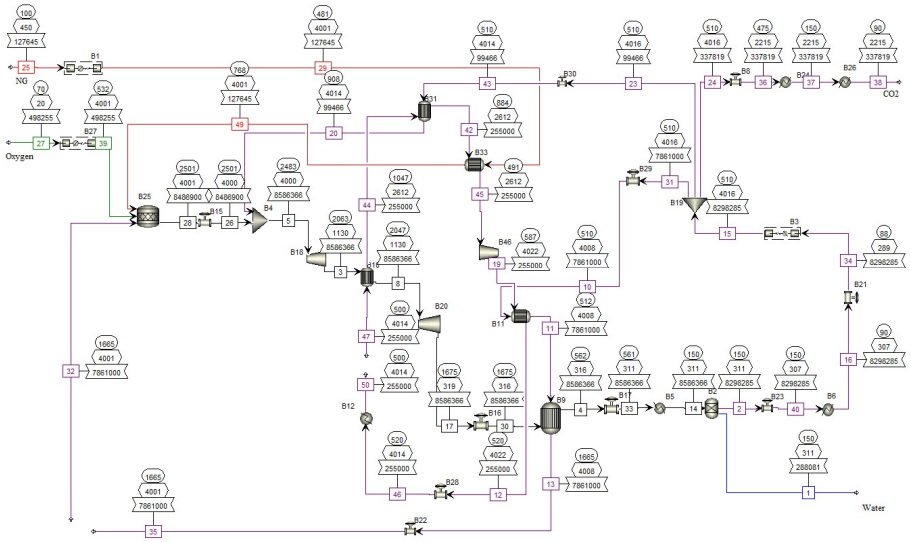

Figure 4. Direct Cycle - NG with CO2 Coolant in Separate Closed Loop

2.2 Turbomachinery Analysis

Approach: Case 5 with NG and CO2 as the coolant was chosen to proceed forward with the turbomachinery analysis. Boundary conditions for the turbomachinery were taken from the system model. Single and dual shaft configurations were evaluated. The same approach was taken for the turbomachinery analysis for the directly heated cycle as with the indirectly heated cycle. No sizing was performed for the CO2 compressor for the regenerative blade loop coolant as it will be an off the shelf reciprocal compressor.

Results/Discussion: Both turbine configurations had similar system performance, but the dual shaft configuration was chosen to provide flexibility during transients and part load operation.

Fuel	Coolant	SCOT PWR Turbine (MW)	SCOT PWR Turbine Efficiency	SCOT PWR Turbine RPM	SCOT CMPR Turbine (MW)	SCOT CMPR Turbine Efficiency	SCOT CMPR Turbine RPM	Steam Turbine (MW)	Steam Cycle Efficiency	Main Compressor (MW)	Main Compressor Efficiency	Main Compressor RPM	Auxiliary Loads (MW)	Heat Input (MW)	Total Power (MW)	Mass Flow Rate (lb/hr)	Cycle Efficiency	Plant Efficiency
NG	Steam	484	88.8%	3600	154	86.4%	4900	167	36.0%	154	83.6%	4900	256	846	549	8,329,825	76.90%	64.89%
Syngas - 91% H2	Steam	561	88.8%	3600	174	86.4%	4900	211	36.5%	174	83.6%	4900	397	1310	549	9,378,270	76.35%	41.91%
Syngas - 39% H2	Steam	537	88.8%	3600	166	86.4%	4900	190	37.5%	166	83.6%	4900	344	1190	549	9,200,275	76.97%	46.17%
NG	CO2	490	88.8%	3600	171	86.4%	4900	158	36.5%	171	83.6%	4900	269	853	549	8,519,099	75.91%	64.40%
NG	CO2 (sep loop)	494	88.8%	3600	173	86.4%	4900	153	36.0%	173	83.6%	4900	269	853	550	8,586,366	75.86%	64.51%
Sygnas - 39% H2	CO2 (sep loop)	537	88.8%	3600	191	86.4%	4900	179	37.5%	191	83.6%	4900	356	1194	551	9,414,349	76.99%	46.17%

Table 4. Final Results of Directly Heated Cycles with Updated Turbomachinery Efficiencies

Two stages were required for the main compressor, and both the generator and compressor turbines are 8 stages. They have a straight through flow configuration, as opposed to the back-to-back configuration of the turbines in the indirectly heated cases because of turbine blade height constraints. The generator turbine operates synchronously with the generator at 3600 RPM. The compressor turbine operates synchronously with the compressor at 4900 RPM.

Both turbines require film cooling of the first stage vane but utilize regenerative cooling for remaining blade rows of the first five stages.

3 Material Compatibility

3.1 Corrosion Coupon Tests (Unstressed State)

Approach: Samples of seven alloys were exposed to 99.995% CO2 at 2900 psig and 750°C for 500 hours. Three replicate samples from the same heat and fabrication sequence were exposed simultaneously to reduce the impact of variability in oxidation rate. Three materials showing low weight gain rates were then selected for microstructural evaluation. The evaluations comprised optical metallography of both exposed and unexposed (control) panels followed by selective examination using scanning electron microscopy (SEM) and elemental analysis using energy dispersive X-ray spectroscopy (EDS).

Results/Discussion: Table 5 summarizes the list of materials tested and the average rate of weight gain for each material in the unstressed and stressed testing.

Component	Material	Form	Material Source	Weight Gain (mg/cm3)	
				Coupons (Unstressed)	C-rings (Stressed)
Housing	HK40	Sand Casting	Metal Samples Co	0.51	0.74
	HK50	Sand Casting	Metal Samples Co	0.34	
	CAFA7	Centrifugal casting	Murali Muralidharan - ORNL		0.55
	DAFA30	Centrifugal casting	Murali Muralidharan - ORNL		1.05
	Haynes 282	Cast Plate	Phil Maziasz – ORNL		0.26
Disk	Waspaloy	Wrought material	Metal Samples Co	0.37	0.27
	Udimet Alloy 720	Wrought material	Metal Samples Co	0.54	
	Alloy 718	Wrought material	Metal Samples Co	0.30	0.23
	Alloy A-286	Wrought material	Metal Samples Co	17.62	
	Rene 41	Wrought material	Metal Samples Co	0.55	
Blade	CMSX-4	Cast test bar (single crystal)	PCC Airfoils, LLC		0.20
	CMSX-8	Cast test bar (single crystal)	PCC Airfoils, LLC		0.09
	PWA 1483	Cast test bar (single crystal)	PCC Airfoils, LLC		0.48
	Rene N4	Cast test bar (single crystal)	PCC Airfoils, LLC		0.13

Table 5. Summary of material compatibility tests

All samples in the unstressed test showed increased mass consistent with the formation of an adherent oxide film. It was also found there was an increasing rate of activity with temperature when compared to previously generated ORNL results. Alloy 718, Waspaloy, and HK40 were chosen for microstructural evaluation. All three alloys showed a surface oxide film approximately 2 μm in thickness. In addition, the two Ni-base alloys also showed some significant

levels of subsurface oxidation with penetrations of approximately 3 μm. This suggests that these materials might be susceptible to spalling and reduced life, especially in high flow velocity regions. Further testing in a dynamic environment is recommended to evaluate this risk.

3.2 C-Ring Exposure Tests (Stressed State)

Approach: The exposure of stressed samples utilized the bottom 5 inches of the autoclave with C-Rings layered in three closely packed levels to achieve an approximately uniform zone (+/- 5°C). Two 500-hour exposures permitted exposure of a total of 30 rings in two batches. Each sample was stressed prior to exposure to either a 75%, 85%, or 95% level of the calculated creep-rupture stress in air at 750°C.

Results/Discussion: The surface condition varied significantly with alloy type, with some spalling of the surface oxide apparent for three of the largest rings (HK40). No cracking was noted in any sample during visual examination. The Fe-base alloys (HK40, CAFA7 and DAFA30) oxidized more quickly than the Ni-Cr alloys. The high aluminum content alloys within the Ni-Cr group did not always produce higher oxidation resistance, but that is not unexpected since an alumina layer would be very slow to develop at the test temperature. A higher temperature oxidation treatment would be required to fully develop a protective alumina layer and which should impart much improved resistance to oxidation and/or carburization. Preliminary measurements of higher carbon concentrations near the surface of some samples are consistent with observations of carburization previously reported. No clear evidence was found of environmentally-assisted crack growth in cross sections of any of the C-ring samples that were exposed.

4 Conclusion

Six indirectly heated SCO2 Brayton cycles were analyzed; 10MWe and 550 MWe plants were evaluated further with turbomachinery sizing and analysis. The predicted cycle efficiencies were 50% and 53%, respectively. Six directly heated cycles were analyzed. The NG cycle utilizing CO2 as the turbomachinery coolant was analyzed further with turbomachinery sizing and analysis. The plant efficiency of the directly heated cycle was 64.5%.

For material compatibility testing, all samples exposed in SCO2 showed some oxidation, the extent of which varied considerably between the alloys tested. Examination of cross sections of the C-ring samples found no evidence of cracking that was due to exposure in the SCO2. The performance of the alumina forming alloys would likely be improved by using a higher temperature (at least 1000°C) pretreatment.

Both the indirectly and directly heated cycles show efficiency improvements over current steam Rankine cycles, and the directly heated cycles show improvements over current NGCC cycles. The higher density of the SCO2 also allows for more compact turbomachinery, reducing capital cost. Combined, these reduce the cost of electricity, and the higher efficiencies reduce CO2 emissions. One of the largest technology gaps is material compatibility in an SCO2 environment. Testing has shown that while there is some oxidation, and further testing recommended in a more representative dynamic environment, an improved pretreatment process could limit the amount of corrosion providing a path forward for alumina forming alloys. The results presented here are relevant to future technology development as they continue to show the environmental and economic benefits of SCO2 Brayton cycles, have further validated turbomachinery technology roadmaps, have provided an initial screening of materials typically used in turbomachinery applications, and have identified the next steps necessary for material selection for these applications.